Frontier molecular orbital analysis of dual fluorescent dyes: predicting two-color emission in *N*-Aryl -1,8-naphthalimides†

Premchendar Nandhikonda, Michael P. Begaye, Zhi Cao and Michael D. Heagy*

Received 28th January 2010, Accepted 28th April 2010
First published as an Advance Article on the web 19th May 2010
DOI: 10.1039/c001912g

A 3 × 3 matrix of disubstituted *N*-aryl-1,8-naphthalimides was synthesized for the evaluation and discovery of dual fluorescence (DF). The matrix elements included for this study were based on a predictive model that is proposed as a seesaw balanced photophysical model. This model serves as a guide to optimize the dual fluorescence emission from *N*-phenyl-1,8-naphthalimdes by appropriate placement of substituent groups at both the 4-position of the *N*-arene as well as the 4′-position of the naphthalene ring. Steady-state fluorescence studies under a variety of solvents indicate that four of the nine dyes in the matrix are dual fluorescent. To provide a more quantitative description of the model, cyclic voltammetry experiments were used to calculate HOMO/LUMO energies of the aromatic components that comprise these DF dyes and give evidence in support for potential mixing of S_1 and S_2 excited states. Given the difficulties in predicting excited state properties such as molecular fluorescence, this ratio of four out of nine "hits' for discovering DF signifies proof of principle for this proposed model and should provide a rational basis for the synthesis of future DF 1,8-naphthalimide systems.

Introduction

While it is highly desirable to predict fluorescence features of organic dyes from first principles, for relatively large molecule systems, the current level of computation cannot obtain the full potential energy surfaces for the ground state and the excited state.[1] Semiempirical methods have made some progress in predicting excited state charge transfer properties using time-dependent density functional theory (TDDFT). For example, this computational method has confirmed the dual fluorescent (DF) properties for dimethylaminobenzonitrile (DMABN) and related compounds.[2] Nevertheless, given the complexities involving solvent, substituent groups, and the underlying photophysical pathways, chemists have resorted principally to combinatorial synthetic approaches to obtain optimal features such as brightness, large Stokes shift, *etc*.[3] A rational approach to the design and synthesis of dyes is preferable since less material is required and fewer optical measurements are needed.

Generally, dual fluorescent molecules can be categorized as either tautomeric systems such as the benzofluroscein class of compounds or TICT systems based on DMABN and its analogues.[4,5] Recently, two-color emission band separation has been improved by exploring the initial and phototautomer states of the 3-hydroxyflavone (3HF) family of compounds.[6] These two-color dyes were developed using an "internal Stark-effect" uniquely applied to their structure. *N*-Arylnaphthalimides, specifically 1,2-, 2,3-, and 1,8-naphthalimides, appear to be a class of fluorescent dyes unlike either category and represent one of the few exceptions to the well-established model of TICT compounds.[7] Within just the past few years, there has been an upsurge in the number of reports on the photophysics and applications of NI based dyes.[8] The two-color emission that certain NI dyes display places them among a select few that exhibit so-called "OR–OR switching" in a reversible excited state.[9] This category of dyes along with electrochromic hydroxyquinoline dyes[10] are particularly useful as probes since they provide internal calibration *via* two-channel output for more accurate analyte detection. Moreover, because the dual fluorescence bands are spread over the entire visible region, the color of the emission appears white and may be applicable as a new lighting source.[11]

Berces and coworkers have studied *N*-substituted-1,8-naphthalimides extensively and reported that two emitting states, S_1 and S_2, are responsible for the short-wavelength (SW) and long-wavelength (LW) fluorescence, respectively.[12] Their identification of the first and second excited singlet states is supported by Hückel MO calculations carried out for the parent 1,8-NI.[12] The calculated electron distributions for the frontier molecular orbitals involving $S_0 \rightarrow S_1$ and $S_0 \rightarrow S_2$ transitions are relevant to coplanar geometries and given in Fig. 1. From these seminal studies, a valence bond description was developed to account for the presence of two excited states in equilibrium. This model depicts the two emitting states with rotational dynamics existing between two predominant conformations. The LW emission results from a coplanar configuration and SW emission results from an orthogonal configuration. While this model provides insights into the causes of dual fluorescence, it does not fully explain why some 1,8-naphthalimide systems display only LW emission while others display SW emission and a few display both Therefore, this paper attempts to provide a more quantitative explanation for DF (and less phenomenological description) by investigating the relative energies of the frontier molecular orbital of *N*-aryl-4-substituted naphthalimides.

In an earlier report, we implemented a synthetic matrix approach to discover DF dyes by preparing a forty-two element

Department of Chemistry, New Mexico Institute of Mining and Technology, Socorro, New Mexico, USA. E-mail: mheagy@nmt.edu

† Electronic supplementary information (ESI) available: NMR spectra. See DOI: 10.1039/c001912g

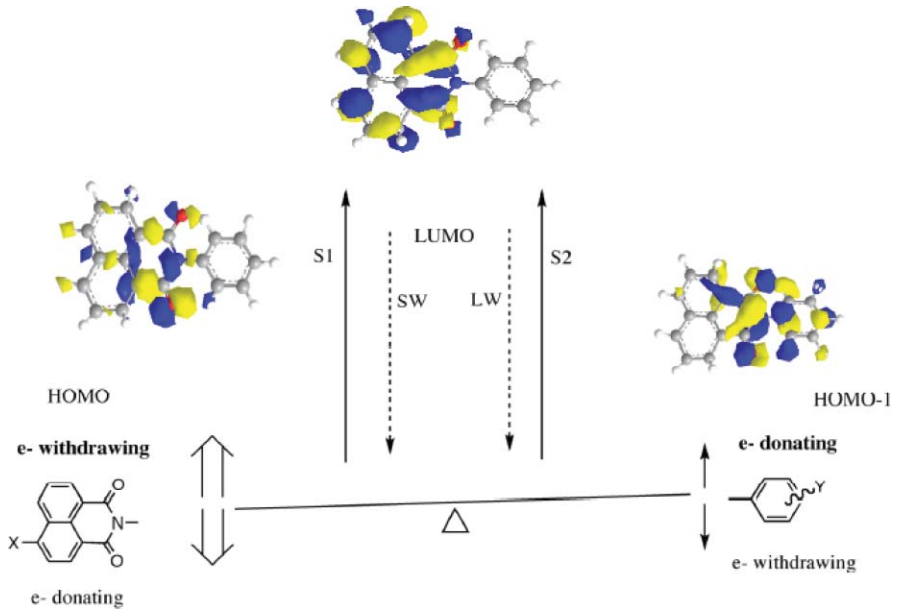

Fig. 1 Relevant molecular orbitals of *N*-phenyl-1,8-naphthalimide scaffold. Seesaw model depicts energies of HOMO and HOMO-1 in their initial calculated positions. With proper arene substituents indicated in bold, the seesaw becomes balanced whereby HOMO-1 gains parity with HOMO energy level thereby promoting both SW and LW emission.

matrix of *N*-aryl-1,8-NI's.[13] From that synthetic matrix of dyes, five indicated a combination of substituents on both the naphthalene component and the arene ring necessary for promoting DF. Based on those findings, we developed a photophysical model (Fig. 1), best described as a seesaw whereby balance between electron donation into the *N*-arene and electron withdrawal from the naphthalimide is required to promote the two-color spectrum. According to this model, electron-withdrawing groups (EWG) on either the naphthalene ring or phenyl ring promote short wavelength (SW) emission by decreasing the energy of the charge transfer; conversely, electron-donating groups (EDG) on both sides are responsible for long wavelength (LW) emission. If, however, the naphthalimide ring has an EDG and the phenyl ring has an EWG, the dye displays LW emission; hence the pronounced arrows on the side of NI. Finally, if an EWG is placed on the naphthalene ring and an electron-releasing group on phenyl, the two states appear to be equalized as evidenced by both SW and LW emission.

To prove the validity of this balanced beam model, we present a more focused nine element matrix that gives a much higher percentage of DF emission. In addition to previously reported optical measurements,[14] experimentally obtained values for HOMO and LUMO energy levels are used as evidence to support the equal mixing of both SW and LW states. As indicated in Fig. 1, electron transfer from the HOMO to the LUMO occurs from the π* orbitals of the carbonyl groups to the naphthalene moiety, in which the electrons of the aniline group do not participate. Orbital densities (obtained *via* computation using Gaussview)[15] for both HOMO and LUMO indicate virtually zero electron density at the aniline group, so electron transfer between these molecular orbitals is consistent with an orthogonal geometry. This excited state is expected to relax *via* radiative decay as SW emission. A comparison between the electron distributions in HOMO-1 and LUMO orbitals, however, indicates that electron density undergoes a longer distance shift from the aniline ring to naphthalene moiety. This S_2 state reverses the direction of the dipole moment in relation to the ground state, thus giving rise to charge-transfer character (ICT) states responsible for solvent stabilized LW fluorescence. Recent efforts have focused on the use of donor groups located on the arenes of *N*-aryl-1,8-naphthalimides to promote LW emission; whereas obtaining two-color emission from NI dyes has been less predictable.[12] Therefore, to promote parity between both excited state populations (S_1 and S_2) necessary for two-color emission, the electronic properties of both aromatic ring systems must be adjusted.

Results and discussions

The 3 × 3 matrix of compounds was prepared using two commercially available compounds, specifically, 4-chloro- and 4-sulfonaphthalic anhydride along with 4-cyanonaphthalic anhydride *via* palladium-catalyzed cyanation of 4-bromonaphthalic anhydride (Scheme 1).[4] These three anhydrides were coupled

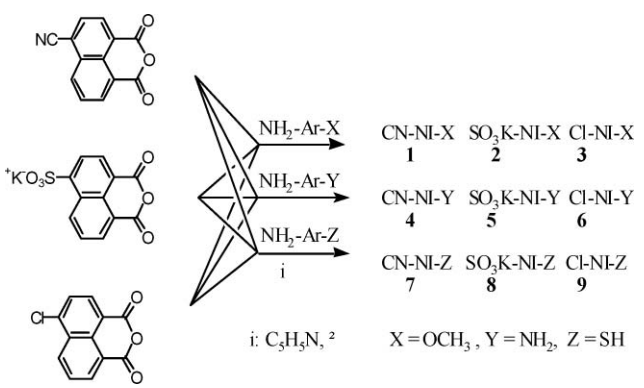

Scheme 1 Synthetic scheme for 3 × 3 matrix elements

with electron-releasing aminoarenes that have either 4-methoxy, 4-amino- or 4-thiol functional groups.

The synthesis of each element of the 3 × 3 matrix involved simple coupling in a 1 : 1 ratio of the 4-substituted naphthalimide with the respective aminoarenes in a minimum amount of pyridine as solvent.

Absorption

In the case of *N*-aryl-1,8-naphthalimides, the overlap with other transitions has been shown to make identification of the $S_0 \rightarrow S_1$ and $S_0 \rightarrow S_2$ transitions difficult. However, based on earlier reports involving *N*-aryl-2,3-naphthalimides of same symmetry (C_2), transitions corresponding to structured absorption bands in the longer wavelength range (*i.e.* 340–360 nm) are tentatively assigned to π–π* transition from HOMO → LUMO.[14] Whereas the next (HOMO-1 → LUMO) transition has been shown to be a less intense band in the shorter wavelength region (*i.e.* 285–340 nm) and corresponds to an (n, π*) state. The intensity of this transition has been shown to increase with increasing charge transfer character.[16] As shown in Fig. 2, the absorption spectra of dyes **1** and **4** show significant absorption for the shorter wavelength region. However, based on the observation that compounds **2** and **6** have relatively low intensity absorption in this region, the increases for **1** and **4** may be due to the nitrile functionality that is common to both naphthalimide components. In either case, all four dyes show absorption intensities in the shorter wave region (285–340 nm) well above baseline beginning at wavelengths greater than 360 nm.

Fluorescence

Of the nine compounds included in this matrix, four displayed the well-separated LW and SW emission bands that fit our criteria for DF dyes (Fig. 2). Fluorescence profile bands for systems that display the two-color phenomena are similar to those we reported earlier and by Berces in that the SW peak is generally more sharp than the broader LW band.[12] This photophysical feature for the SW band has already been ascribed to the S_1 transition whereas the LW band appears to be the result of S_2 emission. For the three cyano-substituted NI systems, both the methoxyarene and aminoarene derivatives displayed two bands with the greatest parity. Because this 3 × 3 matrix varies in both NI substitution as well as arene substitution, the fluorescence profiles can be viewed as being dependent on the electronic properties of both substituents. As illustrated in our model, DF depends on the balance or more appropriately, mixing between HOMO and HOMO-1 energy levels. Substituent groups with greater orbital overlap (*e.g.* C–OR > C–S) are expected to stabilize this excited state extended conformation. Alternatively, SW emission results from the near orthogonal conformation as first introduced by Bérces.[16] For example, none of the thiophenyl derivatives displayed DF; only a single emission band. Sulfur substitution in the form of 4-thiophenyl groups has less overlap with the aromatic ring and is more electropositive than oxygen as in the form of a methoxy group. So its ability to serve as an electron donor is diminished relative to a 4-methoxyarene. Therefore, the 4-methoxyarene systems tend to provide a relatively good ratio (two out of three hits) in our assay for DF dyes. Two of the 4-methoxyarene derivatives, specifically, 4-methoxyphenyl-4-cyano NI (**1**) and 4-methoxyphenyl-4-sulfo NI (**2**) gave distinct two-color emission. The 4-methoxyphenyl-4-cyano NI (**1**) shows the two bands with the greatest parity. Here, the greater orbital overlap with the ether oxygen as the donor group and the arene component may account for the necessary balance to manifest two-color emission. According to ratios of SW to LW fluorescence intensity in Table 1, where $r = \Phi_f^{LW}/(\Phi_f^{SW} + \Phi_f^{LW})$, the contribution of the LW component to the fluorescence (*i.e.* their ratio *r*) increases with *p*-NH_2 substitution.

Table 1 Summary of fluorescence wavelengths and quantum yields

Entry	Excitation λ/nm	Emission λ/nm	ϕ_F (10^{-3})	$r = \phi_F^{LW}/(\phi_F^{SW} + \phi^{LW})$
1	410	521, 603	46, 46	0.50
2	340	369, 512	0.36, 0.28	0.44
3	410	505	7.7	
4	420	520, 576[a]	5.1, 25	0.83
5	340	426	1.3	
6	340	437, 569	2.5, 3.8	0.60
7	410	553	17	
8	340	388	1.6	
9	345	500	2.6	

[a] In the event of a dual fluorescence response, excitation wavelengths were selected in order to maximize the fluorescence intensities of both SW and LW emission. Fluorescence quantum yields relative to quinine sulfate in water. Errors are in the order of ± 5% for quantum yields. The values for this data set were obtained from dichloromethane. (a) Data taken using acetonitrile as solvent. (b) Data taken using acetone as solvent.

HOMO/LUMO energy values

To gain a more quantitative understanding of the frontier molecular orbitals involved, cyclic voltammetry experiments were carried out on the aromatic components that comprise this matrix of dyes. According to the following equations proposed by Gilman,[17]

$$E_{HO} = -E_{OX} \text{ (V, } vs. \text{ AgCl)} - 4.72 \quad (1a)$$

$$E_{LV} = -E_{HO} + E_{\lambda max} \text{ (eV)}, \quad (1b)$$

(or)

$$E_{LV} = -4.42 - E_{Red} \text{ (V, } vs. \text{ Ag/AgCl)}, \quad (2a)$$

$$E_{HO} = -E_{LV} - E_{\lambda max} \text{ (eV)}, \quad (2b)$$

the energy of the highest occupied level E_{HO} and lowest unoccupied level E_{LV} of the dye can be calculated from the oxidation or reduction potential E_{OX} or E_{Red} of the dye, respectively, and the energy $E_{\lambda max}$ (eV), which corresponds to the wavelength of maximum absorption of the dye. The calculated values for the constituent dye components are given in Table 2.[19] These energy levels are portrayed in the diagram below as being virtually separated due to the C_0 spacer inherent to the *N*-aryl-naphthalimide systems (fig. 3).[18] Based on recent studies by Takahashi *et al.* where *N*-aryl-1,8-naphthalimides were shown to behave as molecular dyads using electron-rich *N*-aryl systems, a similar comparison was made by examining the individual building blocks of dyes **1–9**.[14] As noted in their work, it is the Marcus reorganizational energy that brings these separate π-systems and their molecular orbitals into coplanar orientation. Electron transfer is facilitated in these systems by taking advantage of the electron-deficient

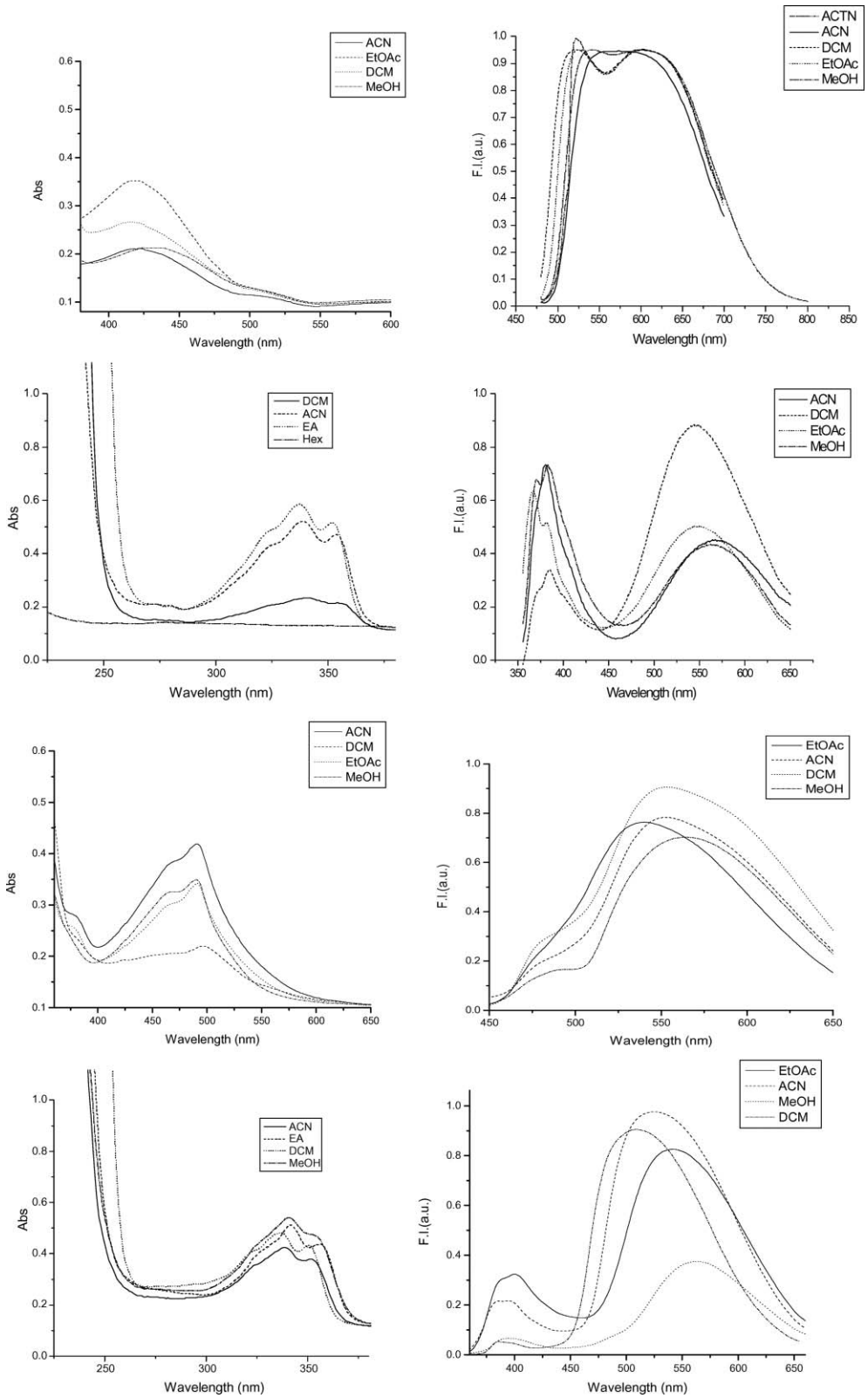

Fig. 2 Absorption and corresponding dual fluorescence spectra of compounds 1, 2, 4, and 6 (1.0×10^{-5} M) in solvents indicated. Fluorescence spectra are normalized to the maximum of each data set. Excitation wavelengths are shown in Table 1.

Table 2 Energy differences (in eV) between HOMO and LUMO for NI–X and arene–Y systems

NI–X HOMO/eV	**NI–X** LUMO/eV	ΔE |**eV**|
SO_3H –6.72	SO_3H –3.20	3.52
CN –6.82	CN –3.05	3.77
Cl –6.87	Cl –3.23	3.64
Ar–Y HOMO/eV	**Ar–Y** LUMO/eV	
SH –5.01	SH –0.66	4.35
OCH_3 –6.47	OCH_3 –2.80	3.67
NH_2 –7.48	NH_2 –3.40	4.08
Ar–Y HOMO/eV	**NI–X** LUMO/eV	
SH –5.01	SO_3H –3.20	1.81
	CN –3.05	1.96
	Cl –3.23	1.59
OCH_3 –6.47	SO_3H –3.20	4.25
	CN –3.05	3.42
	Cl –3.23	3.24
NH_2 –7.48	SO_3H –3.20	4.28
	CN –3.05	4.43
	Cl –3.23	4.25

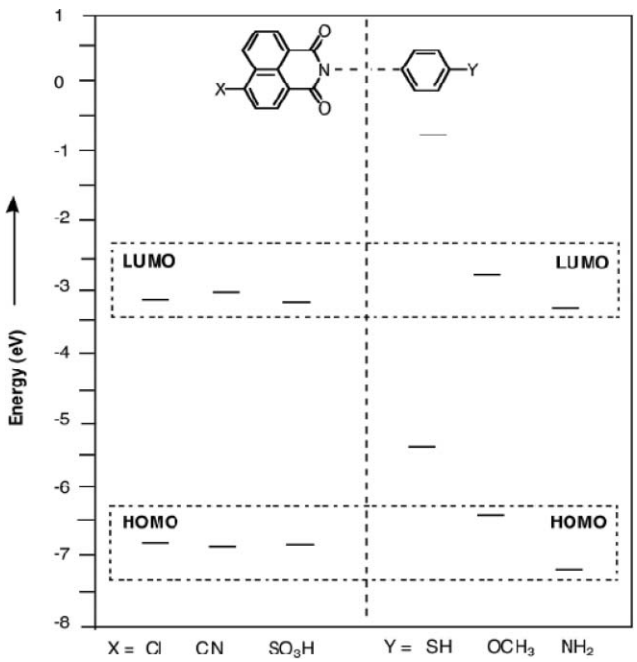

Fig. 3 Comparison between HOMO and LUMO levels of constituent aromatic building blocks based on cyclic voltammetry results. Graph indicates energy proximities of the amino and methoxy arenes to naphthalimides for both HOMO and LUMO levels. The HOMO and LUMO energies of thioarene are well above these levels and indicate a lower probability for coupling between these aromatic systems.

naphthalimide ring relative to the electron-rich arenes. Compared to the first excited singlet state, which has been shown to be mainly the HOMO → LUMO transition, Fig. 1 depicts the S_2 transition where HOMO-1 is localized on the donor arene and the LUMO on the acceptor part (naphthalimide). By inspection of the relative energies of these dyad groups, it appears that both amino and methoxy anilines have similar energy gap differences between their HOMO/LUMO and the HOMO/LUMO of any NI–X group.[20] As shown in Table 2 and depicted in Fig. 3, all of the differences (ΔE eV) for systems other than thioarenes are between 3.5–4.4 eV. Therefore, the probability of electronic coupling between the two states increases and gives rise to emission bands originating from both S_1 and S_2. One exception to this analysis appears to be the aminoarene/sulfonaphthalimide dye **5** which did not display DF despite attempts at temperatures higher than rt.[21] Such exceptions continue to emphasize the difficulty in predicting excited state outcomes of organic dyes.

Conclusion

In closing, a 3 × 3 synthetic matrix was constructed for the discovery of new dual fluorescent compounds. These dyes were examined with the use of cyclic voltammetry and quantum chemical calculations to verify the predictive ability of a photophysical model for substituted *N*-phenyl-1,8-NI. Of the nine compounds compared, four displayed DF phenomena. The dyes obtained from this smaller matrix show an increase in quantum yield (by one order of magnitude) relative to the first generation matrix. Such improvements signify an added refinement in the strategy towards brighter dyes with two-color emission and provide a useful guide for the synthesis of additional DF dyes. Moreover, use of the photophysical model gave far more "hits" than recently reported combinatorial approaches in search of other useful photophysical features (QY, stokes shift, *etc.*).[3] Cyclic voltammetry measurements were used to lend support to this model *via* HOMO/LUMO energies of the individual donor and acceptor building blocks. The Ered values obtained by this analysis provided energy levels that were consistent with the steady state emission spectroscopic features of the nine compounds included in this study. Therefore a more quantitative description of orbital energies is provided for these dyes relative to other dual fluorescent systems.

Given the difficulties in predicting photoemissive properties of excited states, this increased percentage in DF species provides added proof to the prescribed 'see-saw' model necessary for promoting DF Our findings indicate that additional DF systems for NI are best designed with heteroatom donor groups such as nitrogen and oxygen and heteroatom acceptor groups with similar principle quantum number. These findings bode well for future investigations into symmetry-related 2,3-naphthalimide systems. Investigations into these fluorophores are currently under way in our lab. Applications of these DF dyes as luminescent platforms for optical signaling in the field of chemosensors as well as biomarkers are currently under way.

Experimental section

General experimental: in a typical reaction, 1 mmol of the 4-substituted naphthalic anhydride was combined with 1.1 mmol of the 4-substituted aminoarene. The reactants were refluxed in approximately 3–4 mL pyridine for a period of 12 h. Pyridine was removed in the fume hood *via* stream of air and the residue was filtered using a plug of silica gel with the appropriate solvent as found through TLC analysis. Recrystallization was further carried out using ethanol.

General procedure for preparation of 4-cyano-1,8-naphthalic anhydride

4-Bromo-1,8-naphthalic anhydride (3.1 mmol) and tetraethyl ammonium cyanide (7.0 mmol), CuCN (11.0 mmol), $Pd_2(dba)_3$ (0.12 mmol) [tris(dibenzylidene acetone)dipalladium], DPPF (0.48 mmol) (1-diphenylphosphino-1-(di-*tert*-butyl phosphino)-ferrocene were dissolved in 15 mL of anhydrous 1,4-dioxane. The resulting mixture was refluxed in presence of argon gas for 3 h. The reaction mixture was filtered over Celite-521 and the product was purified in 50 : 50 of ethyl acetate and hexane solution.

4-Cyano-*N*-(4′-methoxyphenyl)-1,8-naphthalimide (1). m.p. 180–183 °C; ^{1}H NMR DMSO-d6 δ, 8.61 (dd, J = 7.7 Hz, 2H), 8.37 (d, J = 8.1 Hz, 1H), 8.35 (d, 8.0 Hz, 1H) 8.15 (dd, J_{app} = 7.5 Hz, 1H), 7.29 (d, J = 8.8 Hz, 2H), 7.07 (d, J = 8.5 Hz, 2H) 3.83 (s, 3H)

^{13}C DMSO-d6, δ 164.3, 159.5, 133.3, 132.3, 131.9, 131.7, 130.9, 130.6, 130.5, 129.8, 129.4, 128.7, 123.9, 114.8, 55.7.

IR cm^{-1} ν = 2361, 1707, 1513, 1364, 1238, 1187, 829, 789.

Anal. Calcd. for $C_{20}H_{12}N_2O_3$: C, 73.2; H, 3.66; N, 8.54. Found: C, 72.8; H, 3.74; N, 8.66

4-Sulfo-*N*-(4′-methoxyphenyl-1,8-naphthalimide (2). m.p. 288–290 °C dec; ^{1}H NMR DMSO-d6, δ, 9.30 (d, J = 8.9 Hz, 1H), 8.47 (dd, J = 8.0 Hz, 2H), 8.26 (d, J = 6.9 Hz, 1H), 7.90 (dd, J_{app} = 7.4 Hz, 1H), 7.34 (d, J = 14 Hz, 2H), 7.09 (d, J = 14 Hz, 2H). 3.83 (s, 3H)

^{13}C NMR DMSO-d6 δ, 164.3, 164.1, 159.5, 134.9, 134.7, 131.1, 130.8, 130.7, 130.5, 129.1, 128.9, 127.2, 123.9, 123.2, 115.2, 114.8, 56.0.

IR cm^{-1} ν = 1658, 1514, 1243, 1262, 1196, 1070, 1032, 785, 754,

Anal. Calcd. for $C_{19}H_{13}NSO_6$ K $^{\cdot}2H_2O$: C, 50.0; H, 2.8; N, 3.06 Found: C, 49.7; H, 2.9; N, 3.10

4-Chloro-*N*-(4′-methoxyphenyl)-1,8-naphthalimide (3). m.p. 215–218 °C; ^{1}H DMSO-d6, δ 8.68 (d, J = 8.6 Hz, 1H), 8.42 (d, J = 7.1 Hz, 1H) 8.19 (d, J = 8.3 Hz, 1H), 7.69 (dd, J_{app} = 8.3 Hz, 1H), 7.21 (d, J = 8.5 Hz, 2H), 7.03, (d, J = 8.5 Hz, 2H), 6.89 (d, J = 7.7 Hz, 1H), 3.83 (s, 3H)

^{13}C DMSO-d6, δ 164.9, 163.9, 159.2, 153.3, 134.5, 131.6, 130.7, 129.7, 129.6, 124.5, 122.9, 121.2, 120.0, 114.5, 108.7, 108.5, 55.9.

IR cm^{-1} ν = 1650, 1513, 1240, 1022, 818, 790

Anal. Calcd. for $C_{19}H_{12}NO_3$: C, 75.4; H, 3.9; N, 4.64 Found: C, 75.3; H, 3.6; N, 4.78

4-Cyano-*N*-(4′-aminophenyl)-1,8-naphthalimide (4). m.p. 218–220 °C; ^{1}H NMR DMSO-d6 δ, 8.54 (d, J = 8.0 Hz, 2H), 8.31 (d, J = 7.7 Hz, 1H), 8.20 (d, 7.7 Hz, 1H) 7.99 (dd, J_{app} = 8.0 Hz, 1H), 6.96 (d, J = 8.2 Hz, 2H), 6.65 (d, J = 8.5 Hz, 2H)

^{13}CDMSO-d6, δ, 163.9, 149.1, 132.2, 131.9, 131.5, 130.5, 130.1, 129.8, 129.8, 129.7, 129.5, 129.4, 129.3, 129.3, 124.2, 124.1, 123.3.

IR cm^{-1} ν = 2359, 1709, 1654, 1514, 1374, 1237, 1168, 834, 783.

Anal. Calcd. for $C_{19}H_{11}N_3O_2$: C, 76.3; H, 3.68; N, 13.4: Found: C, 76.7; H, 3.74, N, 13.2.

4-Sulfo-*N*-(4′-aminophenyl-1,8-naphthalimide (5). m.p. 269–272 °C; ^{1}H DMSO-d6 δ 9.38 (d, J = 8.6 Hz, 1H) 8.51–8.45 (m, 2H), 8.27 (d, J = 7.4 Hz, 1H), 7.90 (t, J = 7.4, 1H), 7.44 (d, J_{app} = 8.8 Hz, 2H), 7.34 (d, J = 8.6 Hz, 2H)

^{13}C DMSO-d6 δ 164.3, 163.9, 151.2, 135.9, 135.2, 134.9, 133.8, 131.0, 130.9, 129.2, 128.4, 127.3, 125.5, 123.6, 123.0, 122.1

IR cm^{-1} ν = 1161, 1514, 1242, 1167, 1032, 751, 657.

Anal. Calcd. for $C_{18}H_{12}N_2SO_5$: C, 58.7; H, 3.26; N, 7.60. Found: C, 58.3; H, 3.03, N, 7.59

4-Chloro-*N*-(4′-aminophenyl)-1,8-naphthalimide (6). m.p. 234–236 °C dec; ^{1}H DMSO -d6, δ 8.62 (d, J = 8.6 Hz, 1H), 8.57 (d, J = 8.0 Hz, 1H), 8.42 (d, J = 8.0 Hz, 1H), 8.10–8.00 (m, 2H), 6.99 (d, J = 8.5 Hz, 2H), 6.66 (d, J = 8.6 Hz, 2H), 5.25 (s, 2H)

^{13}C DMSO-d6 δ 164.1, 163.8, 149.2, 137.8, 132.1, 131.4, 130.5, 129.7, 129.2, 129.1, 129.0, 128.2, 124.1, 123.9, 122.7, 114.3.

IR cm^{-1} ν = 1712, 1662, 1303, 1009, 771, 751.

Anal. Calcd. for $C_{18}H_{11}N_2O_2Cl$: C, 67.1; H, 3.42; N, 8.69 Found: C, 66.8; H, 3.38, N, 8.70

4-Cyano-*N*-(4′-thiophenyl)-1,8-naphthalimide (7). m.p. 202–204 °C; ^{1}H NMR DMSO-d6 δ, 8.64–8.56 (m, 4H), 8.13 (t, J = 7.5 Hz, 1H), 7.76 (d, 7.7 Hz, 2H) 7.48 (d, J = 8.0 Hz, 2H)

^{13}C DMSO-d6, δ 163.6, 163.2, 146.3, 136.5, 134.4, 132.4, 131.3, 131.1, 130.7, 130.6, 129.8, 128.0, 127.9, 116.7, 114.7.

IR cm^{-1} ν = 2360, 1677, 1648, 1561, 1345, 1228, 790, 738.

Anal. Calcd. for $C_{19}H_{10}N_2SO_2$: C, 69.1; H, 3.03; N, 8.48. Found: C, 68.8; H, 3.22; N, 8.45

4-Sulfo-*N*-(4′-thiophenyl)-1,8-naphthalimide (8). m.p. 228–231 °C dec; ^{1}H DMSO-d6 δ 9.31 (d, J = 8.5 Hz, 1H), 8.49 (pseudo t, J = 7.8 Hz, 2H), 8.25 (d, J = 7.4 Hz, 1H) 7.91 (dd, J_{app} = 7.4 Hz, 1H), 7.75 (d, J = 8.5 Hz, 2H), 7.53 (d, J = 8.5 Hz, 2H)

^{13}C DMSO-d6, δ 164.4, 164.1, 150.6, 134.9, 134.7, 131.1, 130.8, 129.1, 128.9, 128.3, 127.4, 125.8, 125.5, 123.9, 123.2, 115.2.

IR cm^{-1}, ν = 1661, 1371, 1240, 1192, 1068, 1042, 783, 753.

Anal. Calcd. for $C_{18}H_{11}NS_2O_5$ K·3H_2O: C, 45.2; H, 2.32; N, 4.84. Found: C, 45.2; H, 2.24; N, 4.76.

4-Chloro-*N*-(4′-thiophenyl)-1,8-naphthalimide (9). m.p. 226–228 °C dec; ^{1}H DMSO-d6 δ 8.64 (d, J = 8.2 Hz, 1H), 8.42 (d, J = 7.4 Hz, 1H), 8.18 (d, J = 7.9 Hz, 1H), 7.67 (dd, J_{app} = 8.5 Hz, 1H), 7.46 (s, 2H), 7.18 (d, J = 7.5 Hz, 2H), 7.03 (d, J = 9.1 Hz, 2H), 6.87 (d, J = 8.6 Hz, 1H).

^{13}C NMR DMSO-d6 δ, 164.0, 163.9, 137.4, 132.9, 131.6, 131.3, 131.1, 130.9, 130.5, 130.3, 129.6, 128.3, 128.2, 124.4, 124.1, 115.7

IR cm^{-1}, ν = 1656, 1583, 1512, 1365, 1238, 1173, 818, 789.

Anal. Calcd. for $C_{18}H_{10}NSO_2Cl$: C, 63.7; H, 3.11; N, 4.13 Found: C, 63.4; H, 3.03; N, 4.10.

Acknowledgements

The authors wish to thank NIH-NIGMS for support.

Notes and references

1 Q. Peng, Y. Yi, Z. Shuai and J. Shao, *J. Am. Chem. Soc.*, 2007, **129**, 9333–9339.
2 C. J. Jödicke and H. P. Lüthi, *J. Am. Chem. Soc.*, 2003, **125**, 252–264.
3 (*a*) N. S. Finney, *Curr. Opin. Chem. Biol.*, 2006, **10**, 238–245; (*b*) M.-S. Scheidel, C. A. Briehn and P. Bäuerle, *Angew. Chem., Int. Ed.*, 2001, **40**, 4677–4679; (*c*) T. Hirano, K. Hiromoto and H. Kagechika, *Org. Lett.*, 2007, **9**, 1315–1318.
4 Z. Grabowski, K. Rotkiewicz and W. Rettig, *Chem. Rev.*, 2003, **103**, 3899–4031. A notable exception includes,; H. Bettermann, M. Bienioschek, H. Ippendorf and H.-D. Martin, *Angew. Chem., Int. Ed. Engl.*, 1992, **31**, 1042–1043.

5 Inoue has classified 11 distinct dual fluorescent systems. With the exclusion of excimer/exciplex formation, these systems may also be simplied to either tautomeric or conformational changes. Y. Inoue, P. Jiang, E. Tsukada, T. Wada, H. Shimizu, A. Tai and M. Ishikawa, *J. Am. Chem. Soc.*, 2002, **124**, 6942–6949.
6 (*a*) A. S. Klymchenko and A. P. Demchenko, *J. Am. Chem. Soc.*, 2002, **124**, 12372–12379; (*b*) (1) A. S. Klymchenko, T. Ozturk and A. P. Demchenko, *Tetrahedron Lett.*, 2002, **43**, 7079–7082; (*c*) A. S. Klymchenko, T. Ozurk, V. G. Pivovarenko and A. P. Demchenko, *Tetrahedron Lett.*, 2001, **42**, 7967–7970.
7 (*a*) A. Demeter, T. Berces, L. Biczok, V. Wintgens, P. Valat and J. Kossanyi, *J. Phys. Chem.*, 1996, **100**, 2001–2011; (*b*) A. Demeter, T. Berces, L. Biczok, V. Wintgens, P. Valat and J. Kossanyi, *J. Chem. Soc., Faraday Trans.*, 1994, **90**, 2635–2641.
8 (*a*) S. Abad, M. Kluciar, M. A. Miranda and U. Pischel, *J. Org. Chem.*, 2005, **70**, 10565–10568; (*b*) R. Badugu, *J. Fluoresc.*, 2005, **15**, 71–83; (*c*) D. W. Cho, M. Fujitsuka, K. H. Choi, M. J. Park, U. C. Yoon and T. Majima, *J. Phys. Chem. B*, 2006, **110**, 4576–4582; (*d*) A. L. Koner, J. Schatz, W. M. Nau and U. Pischel, *J. Org. Chem.*, 2007, **72**, 3889–3895; (*e*) Z. Z. Li, C. G. Niu, G. M. Zeng, Y. G. Liu, P. F. Gao, G. Huang and Y. Mao, *Sens. Actuators, B*, 2006, **114**, 308–315; (*f*) J. L. Magalhaes, R. V. Pereira, E. R. Triboni, P. Berci, M. H. Gehlen and F. C. Nart, *J. Photochem. Photobiol., A*, 2006, **183**, 165–170; (*g*) R. Parkesh, T. C. Lee and T. Gunnlaugsson, *Org. Biomol. Chem.*, 2007, **5**, 310; (*h*) F. M. Pfeffer, A. M. Buschgens, N. W. Barnett, T. Gunnlaugsson and P. E. Kruger, *Tetrahedron Lett.*, 2005, **46**, 6579–6584; (*i*) O. V. Prezhdo, B. V. Uspenskii, V. Prezhdo, W. Boszczyk and Distanov, *Dyes Pigm.*, 2007, **72**, 42–46; (*j*) M. Tasior, D. T. Gryko, M. Cembor, J. S. Jaworski, B. Ventura and L. Flamigni, *New J. Chem.*, 2007, **31**, 247–259; (*k*) M. E. Vazquez, J. B. Blanco and B. Imperiali, *J. Am. Chem. Soc.*, 2005, **127**, 1300–1306; (*l*) M. E. Vazquez, J. B. Blanco, S. Salvadori, C. Trapella, R. Argazzi, S. D. Bryant, Y. Jinsmaa, L. H. Lazarus, L. Negri, E. Giannini, R. Lattanzi, M. Colucci and G. Balboni, *J. Med. Chem.*, 2006, **49**, 3653–3658; (*m*) Z. Xu, Y. Xiao, X. Qian, J. Cui and D. Cui, *Org. Lett.*, 2005, **7**, 889–892; (*n*) Z. Xu, X. Qian and J. Cui, *Org. Lett.*, 2005, **7**, 3029–3032; (*o*) Z. C. Xu, X. Qian, J. A. Cui and R. Zhang, *Tetrahedron*, 2006, **62**, 10117–10122; (*p*) H. X. Yang, X. L. Wang, X. M. Wang and L. H. Xu, *Dyes Pigm.*, 2005, **66**, 83–87.
9 A. Demchenko, *Lab Chip*, 2005, **5**, 1210–1223.
10 (*a*) V. V. Shynkar, A. S. Klymchenko, E. Piemont, A. P. Demchenko and Y. Mely, *J. Am. Chem. Soc.*, 2004, **108**, 8151; (*b*) A. S. Klymchenko and A. P. Demchenko, *J. Am. Chem. Soc.*, 2002, **124**, 12372–12379.
11 (*a*) H. Okamoto, K. Satake and M. Kimura, *ARKIVOC*, 2007, **8**, 112–123; (*b*) Y. Yang, M. Lowry, C. M. Schowalter, S. O. Fakayode, J. O. Escobedo, X. Xu, H. Zhang, T. J. Jensen, F. R. Fronczek, I. M. Warner and R. M. Strongin, *J. Am. Chem. Soc.*, 2006, **128**, 14081–14092.
12 (*a*) A. Demeter, T. Berces, L. Biczok, V. Wintgens, P. Valat and J. Kossanyi, *J. Phys. Chem.*, 1996, **100**, 2001–2011; (*b*) A. Demeter, T. Berces, L. Biczok, V. Wintgens, P. Valat and J. Kossanyi, *New J. Chem.*, 1996, **20**, 1149–1158.
13 H. Cao, V. Chang, R. Hernandez and M. D. Heagy, *J. Org. Chem.*, 2005, **70**, 4929–4934.
14 P. Nandhikonda, M. Begaye, Z. Cao and M. Heagy, *Chem. Commun.*, 2009, 4941–4943.
15 M. J. Frisch, G. W. Trucks, H. B. Schlegel, G. E. Scuseria, M. A. Robb, J. R. Cheeseman, J. A. Montgomery, Jr., T. Vreven, K. N. Kudin, J. C. Burant, J. M. Millam, S. S. Iyengar, J. Tomasi, V. Barone, B. Mennucci, M. Cossi, G. Scalmani, N. Rega, G. A. Petersson, H. Nakatsuji, M. Hada, M. Ehara, K. Toyota, R. Fukuda, J. Hasegawa, M. Ishida, T. Nakajima, Y. Honda, O. Kitao, H. Nakai, M. Klene, X. Li, J. E. Knox, H. P. Hratchian, J. B. Cross, V. Bakken, C. Adamo, J. Jaramillo, R. Gomperts, R. E. Stratmann, O. Yazyev, A. J. Austin, R. Cammi, C. Pomelli, J. Ochterski, P. Y. Ayala, K. Morokuma, G. A. Voth, P. Salvador, J. J. Dannenberg, V. G. Zakrzewski, S. Dapprich, A. D. Daniels, M. C. Strain, O. Farkas, D. K. Malick, A. D. Rabuck, K. Raghavachari, J. B. Foresman, J. V. Ortiz, Q. Cui, A. G. Baboul, S. Clifford, J. Cioslowski, B. B. Stefanov, G. Liu, A. Liashenko, P. Piskorz, I. Komaromi, R. L. Martin, D. J. Fox, T. Keith, M. A. Al-Laham, C. Y. Peng, A. Nanayakkara, M. Challacombe, P. M. W. Gill, B. G. Johnson, W. Chen, M. W. Wong, C. Gonzalez and J. A. Pople, *GAUSSIAN 03 (Revision B.03)*, Gaussian, Inc., Wallingford, CT, 2004.
16 V. Wintgens, P. Valat, J. Kossanyi, A. Demeter, L. Biczcok and T. Berces, *J. Photochem. Photobiol., A*, 1996, **93**, 109–117.
17 P. B. Gilman, Jr., *Photogr. Sci. Eng.*, 1974, **18**, 475.
18 T. Sakamoto and K. Oshawa, *J. Chem. Soc., Perkin Trans. 1*, 1999, 2323–2326.
19 J. Xiang, C. Chen, B. Zhou and G. Xu, *Chem. Phys. Lett.*, 1999, **315**, 371–378.
20 V. Wintgens, P. Valat, J. Kossanyi, A. Demeter, L. Biczcok and T. Berces, *J. Photochem. Photobiol., A*, 1996, **93**, 109–117.
21 (*a*) A. C. Benniston and A. Harriman, *Chem. Soc. Rev.*, 2006, **35**, 169–179; (*b*) 22. P. Valat, V. Wintgens, J. Kossanyi, L. Biczók, A. Demter and T. Bérces, *Helv. Chim. Acta*, 2001, **84**, 2813–2832.